A pair of peptides inhibits seeding of the hormone transporter transthyretin into amyloid fibrils

Received for publication, August 7, 2018, and in revised form, January 22, 2019 Published, Papers in Press, February 7, 2019, DOI 10.1074/jbc.RA118.005257

Lorena Saelices[‡], Binh A. Nguyen[‡], Kevin Chung[‡], Yifei Wang[‡], Alfredo Ortega[‡], Ji H. Lee[‡], Teresa Coelho[§], Johan Bijzet[¶], Merrill D. Benson[‖], and David S. Eisenberg[‡1]

From the [‡]Departments of Biological Chemistry and Chemistry and Biochemistry, Howard Hughes Medical Institute, UCLA-DOE Institute, Molecular Biology Institute, UCLA, Los Angeles, California 90095-1570, the [§]Neurophysiology Department and Corino de Andrade Unit, Hospital Santo António, Centro Hospitalar do Porto, Porto 4099-001, Portugal, the [¶]Department of Rheumatology and Clinical Immunology, University Medical Center Groningen, Groningen, 9713 GZ, The Netherlands, and the [‖]Department of Pathology and Laboratory Medicine, Indiana University School of Medicine, Indianapolis, Indiana 46202

Edited by Paul E. Fraser

The tetrameric protein transthyretin is a transporter of retinol and thyroxine in blood, cerebrospinal fluid, and the eye, and is secreted by the liver, choroid plexus, and retinal epithelium, respectively. Systemic amyloid deposition of aggregated transthyretin causes hereditary and sporadic amyloidoses. A common treatment of patients with hereditary transthyretin amyloidosis is liver transplantation. However, this procedure, which replaces the patient's variant transthyretin with the WT protein, can fail to stop subsequent cardiac deposition, ultimately requiring heart transplantation. We recently showed that preformed amyloid fibrils present in the heart at the time of surgery can template or seed further amyloid aggregation of native transthyretin. Here we assess possible interventions to halt this seeding, using biochemical and EM assays. We found that chemical or mutational stabilization of the transthyretin tetramer does not hinder amyloid seeding. In contrast, binding of the peptide inhibitor TabFH2 to *ex vivo* fibrils efficiently inhibits amyloid seeding by impeding self-association of the amyloid-driving strands F and H in a tissue-independent manner. Our findings point to inhibition of amyloid seeding by peptide inhibitors as a potential therapeutic approach.

Transthyretin amyloidosis (ATTR)[2] is a fatal disease caused by the abnormal aggregation of the protein transthyretin (TTR). TTR, a transporter of retinol and thyroxine in blood, cerebrospinal fluid, and the eye, is secreted by the liver, choroid plexus, and retinal epithelium, respectively. TTR amyloid deposits are found in virtually every organ of ATTR patients, but the heart and nerves are often the first to fail. Although more than 140 known hereditary mutations in the *ttr* gene result in an early onset of the disease, WT TTR is found not only co-depositing with mutant TTR in hereditary ATTR cases but also in sporadic cases in which only WT TTR is present. WT ATTR, or senile systemic amyloidosis, manifests as an age-related disease, and is often overlooked and underdiagnosed (1, 2).

The current standard of care for hereditary cases is liver transplantation, which does not always cure the condition. Through this procedure, most of the circulating mutant TTR is replaced with the WT form that is secreted by the implanted liver. However, this surgery is not sufficient to stop amyloid cardiac deposition in many patients who require heart transplantation a few years later. Our recent studies suggest the reason for such continued cardiomyopathy: pre-formed TTR fibrils present in cardiac tissues of ATTR patients at the time of surgery have the capacity to catalyze or *seed* fibril aggregation of WT TTR that is secreted by the implanted liver (3).

The stabilization of the functional nonamyloidogenic form of transthyretin is currently under clinical assessment. The functional and most abundant form of TTR is tetrameric, with a hydrophobic central tunnel that binds thyroxine. Kelly and colleagues (4) have established that conversion of native transthyretin to amyloid fibrils is preceded by dissociation of tetrameric TTR to monomers, which then undergo a conformational change and form fibrils. Based on this premise, extensive biochemical studies have led to the discovery of compounds such as tafamidis and diflunisal that bind within the hydrophobic central tunnel of TTR and stabilize the native structure, inhibiting its aggregation *in vitro* (5–7). These two ligands stabilize tetrameric transthyretin *in vivo* and delay the progression of disease in many patients. However, the efficacy of these ligands is reduced when administered at late stages of the disease (8, 9).

In our recent studies, we have developed and optimized peptide inhibitors that are designed to cap the tip of TTR fibrils and block further amyloid aggregation (3, 10). This structure-based drug design strategy started with the identification of two amyloid-driving segments of transthyretin: β-strands F and H (10). We then determined the structures of the two segments in their amyloid state and designed peptide inhibitors that block self-

This work was supported by Amyloidosis Foundation Grant 20160759 and 20170827, National Institutes of Health Grant R01-AG048120, and The Howard Hughes Medical Institute. The authors and UCLA have filed an international patent application for the TTR inhibitors (number PCT/US17/40103). D. S. E. is an advisor and equity holder of ADRx, Inc. L. S. is a consultant of ADRx, Inc. The content is solely the responsibility of the authors and does not necessarily represent the official views of the National Institutes of Health.

[1] To whom correspondence should be addressed: Howard Hughes Medical Institute, UCLA-DOE Institute, Departments of Biological Chemistry and Chemistry and Biochemistry, Molecular Biology Institute, Box 951570, UCLA, Los Angeles, CA 90095-1570. Tel.: 310-825-3754; E-mail: david@mbi.ucla.edu.

[2] The abbreviations used are: ATTR, transthyretin amyloidosis; TTR, transthyretin; ThT, thioflavin T; BisTris, 2-[bis(2-hydroxyethyl)amino]-2-(hydroxymethyl)propane-1,3-diol.

association and protein aggregation *in vitro*. This first generation of inhibitors was further optimized in a second study (3).

Amyloid seeding offers a potential therapeutic target to be explored. Clinical observations indicate that amyloid seeding greatly contributes to ATTR pathogenesis (11). In our previous study, we found that tetramer stabilizers do not inhibit amyloid seeding catalyzed by amyloid fibrils extracted from an ATTR-D38A patient (3). In contrast, our peptide inhibitors halted this process. Here we expand our studies by evaluating the efficacy of both tetramer stabilization and peptide inhibitors in blocking amyloid seeding of ATTR fibrils extracted from affected tissue of several types.

Results

Tetramer stabilization by ligands does not inhibit TTR amyloid formation induced by ATTR-D38A ex vivo seeds

We previously found that the presence of tafamidis or diflunisal at 180 μM is not sufficient to prevent amyloid seeding of WT TTR catalyzed by ATTR fibrils extracted from the explanted heart of an ATTR-D38A patient (3). Although ATTR-D38A patients manifest slow progressive polyneuropathy and autonomic symptoms similar to the most common form of hereditary ATTR, ATTR-V30M, they also develop cardiac dysfunction (12). Here we expand our previous study by evaluating the effect of these ligands at various concentrations.

We first confirmed the ability of tafamidis and diflunisal to inhibit protein aggregation in the absence of seeds. Consistent with previous studies, we found that both tafamidis and diflunisal efficiently inhibit WT TTR aggregation *in vitro* under acidic conditions in the absence of seeds (Fig. 1, *a* and *b*) (5–7). For these aggregation assays, we incubated 1 mg/ml of recombinant WT TTR with increasing amounts of stabilizers at pH 4.3 and monitored protein aggregation both by absorbance at 400 nm and immunodot blot of the insoluble fraction, as we previously described (10). After 4 days in the absence of inhibitor, virtually the total amount of TTR present was converted to aggregates. In the presence of either tafamidis or diflunisal, TTR aggregation was diminished in a dose-dependent manner (Fig. 1, *a* and *b*).

We next studied the effect of various concentrations of tafamidis and diflunisal on protein aggregation in the presence of ATTR-D38A *ex vivo* seeds. In our previous study, we observed that the addition of fibril seeds extracted from ATTR cardiac tissue accelerates aggregation not only of WT TTR at pH 4.3 but also monomeric TTR under physiological conditions (3). Additionally, we tested the effect of tafamidis and diflunisal at 180 μM on amyloid seeding and found that this concentration was not sufficient to hinder the process. Here we evaluate the effect of these ligands at various concentrations (Fig. 1, *c–f*). For this assay, we incubated 0.5 mg/ml of recombinant WT TTR with 30 ng/μl of ATTR-D38A *ex vivo* seeds and increasing amounts of ligands. We monitored fibril formation for 24 h by thioflavin T fluorescence (ThT), by immunodot blot of the insoluble fraction (Fig. 1, *c–f*), and by protein quantification of insoluble fractions (Fig. 1*g*), as we previously described (10). We found that these ligands did not reduce or delay seeded fibril formation even at ligand concentrations that resulted in full inhibition of unseeded TTR aggregation (Fig. 1).

Tetramer stabilization does not inhibit TTR amyloid formation induced by any of the ATTR ex vivo seeds studied

In our previous study, we report that our specimen obtained from an ATTR-D38A patient contains type B ATTR amyloid fibrils made of full-length TTR (3, 13). To rule out the possibility of pathology-based specificity, we analyzed seeding inhibition by ligands with seven additional ATTR samples (Fig. 2). For this assay, we incubated 0.5 mg/ml of recombinant WT TTR with 30 ng/μl of ATTR *ex vivo* seeds in the presence or absence of 180 μM stabilizers. We monitored fibril formation by quantifying the protein content in the insoluble fraction after 24 h of incubation at 37 °C. As in our ATTR-D38A experiments, we found that the addition of tafamidis or diflunisal did not reduce the accumulation of insoluble material in the presence of seeds extracted from any of the other seven ATTR cardiac specimens. These findings suggest that tetramer stabilization by ligands may not be an effective strategy to halt amyloid seeding under the studied conditions.

T119M-derived stabilization fails to inhibit amyloid seeding

We then evaluated tetramer stabilization by mutagenesis, analyzing the effect of the T119M TTR variant on amyloid seeding. This variant exhibits high tetrameric stability resulting in a significant delay of the onset of hereditary neuropathic ATTR in patients who carry both *ttr*-V30M and *ttr*-T119M genes (5, 14, 15). Although a sample containing 1 mg/ml of recombinant T119M variant remained soluble after days of incubation at a low pH that causes native TTR to dissociate (10) (Fig. 3*a*), the addition of 30 ng/μl of ATTR-D38A *ex vivo* seeds to 0.5 mg/ml of recombinant T119M did result in seeded fibril formation (Fig. 3*b*). Notably, unlike T119M, the TTR variant T119W, which blocks self-association of strand H (10), did show a significant decrease in protein fibril formation upon seeding (Fig. 3*b*). We also found that although *ex vivo* seeds caused the aggregation of a TTR variant that blocks self-association of strand F, S85P/E92P, the lag phase was significantly longer (Fig. 3, *b* and *c*). Consistent with our previous work (3), these findings suggest that blocking self-association of amyloidogenic TTR segments may be an effective approach to stop fibril formation when ATTR amyloid seeds are present.

TabFH2 halts amyloid seeding caused by ex vivo seeds extracted from all ATTR samples evaluated

In a previous study, we developed peptide inhibitors that were designed to cap the tip of amyloidogenic segments of TTR in their amyloid state (10). Recently, we have shown that the optimized peptide inhibitor TabFH2 blocks amyloid seeding driven by fibrils extracted from the explanted heart of a patient who carries the hereditary mutation ATTR-D38A (3). Note that TabFH2 is a mixture of two peptides, TabF2 and TabH2, which target the two amyloid-driving segments of transthyretin (3, 10). To better compare the efficacy of the peptide inhibitor TabFH2 with tafamidis and diflunisal, we evaluated TabFH2 with the same set of assays. We first found that TabFH2 inhibits

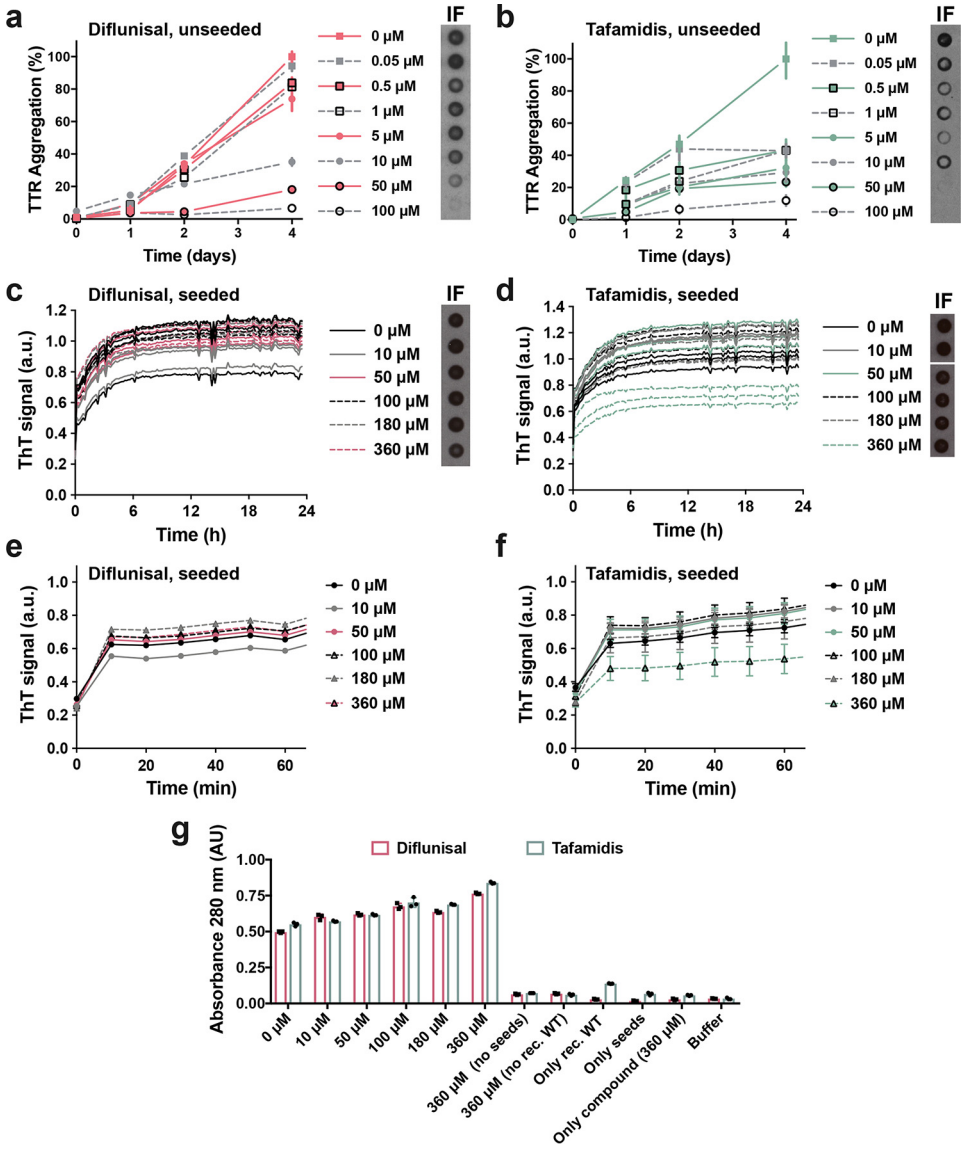

Figure 1. Tetramer stabilizers inhibit TTR aggregation in the absence of seeds and fail to inhibit amyloid seeding caused by ATTR-D38A *ex vivo* seeds. *a* and *b,* inhibition assay of TTR aggregation in the absence of seeds, measured by absorbance at 400 nm. Increasing amounts of diflunisal (*a*) or tafamidis (*b*) were added to 1 mg/ml of recombinant WT TTR and the sample was incubated for 4 days at pH 4.3. Absorbance measured after 4 days of incubation in the absence of ligand was considered 100% aggregation because no soluble TTR was detected. $n = 3$, error bars, S.D. *Right insets*, full inhibition of TTR aggregation by diflunisal (*a*) or tafamidis (*b*) was confirmed by anti-TTR dot blot of insoluble fractions (*IF*) collected by centrifugation. *c* and *d,* inhibition assay of amyloid seeding at pH 4.3, monitored by ThT fluorescence. Increasing amounts of diflunisal (*c*) or tafamidis (*d*) were added to 0.5 mg/ml of recombinant WT TTR and ATTR-D38A seeds. All replicates are shown, $n = 3$. *a.u.*, arbitrary units. *Insets*, anti-TTR dot-blot of insoluble fractions. All samples were spotted onto the same nitrocellulose membrane and subjected to the same procedure; splicing was needed for presentation purposes. *e* and *f,* short-time view of the lag phase of *c* and *d,* respectively. $n = 3$, *error bars*, S.D. *g,* protein content quantification of the insoluble fractions collected from *c* and *d,* measured by 280 nm absorbance. *AU*, absorbance units. Notice that tafamidis at only its highest concentration tested (360 μM) results in a significant reduction of ThT signal (*d*). However, this reduction does not correlate with a reduction of protein content in the insoluble fraction (*g*). Diflunisal treatment did not inhibit amyloid seeding of TTR under tested conditions (*c* and *g*).

TTR aggregation in the absence of ATTR seeds (Fig. 4*a*). For this assay, we incubated 1 mg/ml of recombinant WT TTR with increasing amounts of TabFH2 and monitored protein aggregation for 4 days by absorbance at 400 nm, and visualized the insoluble fraction by immunodot blot, as described above. In addition, we analyzed the inhibitory effect of TabFH2 in our amyloid seeding assays, using the same conditions as in the preceding experiment (Fig. 1, *c–f*): we incubated 0.5 mg/ml of recombinant WT TTR with 30 ng/μl of ATTR-D38A seeds and TabFH2 at various concentrations, for 24 h (Fig. 4, *b–d*). We found that TabFH2 completely inhibits TTR amyloid seeding at concentrations higher than 180 μM with an intermediate effect at lower doses. Longer incubation resulted in similar results (Fig. 4*e*). Altogether, our results indicate that TabFH2 inhibits TTR aggregation when seeded by *ex vivo* patient amyloid fibrils, in a dose-dependent manner (Fig. 4).

We next examined the effectiveness of TabFH2 inhibitors in other pathological cases, by evaluating its inhibitory activity on our additional ATTR *ex vivo* samples (Fig. 5). For this assay, we incubated 0.5 mg/ml of recombinant WT TTR with 30 ng/μl of ATTR *ex vivo* seeds extracted from a total of 9 patients, in the presence or absence of 180 or 360 μM TabFH2. We monitored

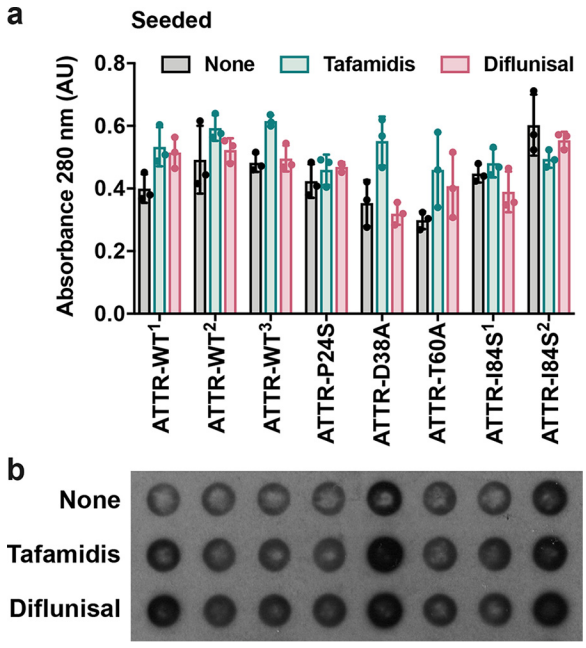

Figure 2. Tetramer stabilizers do not inhibit amyloid seeding caused by any of the cardiac samples analyzed. *a,* inhibition assay of amyloid seeding of *ex vivo* seeds incubated with recombinant WT transthyretin in the absence or presence of 180 μM tafamidis or 180 μM diflunisal. After 24 h of incubation at pH 4.3, the insoluble fraction was collected, and protein content was quantified by absorbance at 280 nm. Consistent with the results observed in Fig. 1, the addition of diflunisal or tafamidis does not result in an apparent reduction of amyloid seeding. *AU*, absorbance units. *b,* anti-TTR dot-blot of the insoluble fractions collected from *a,* shows that tetramer stabilizers do not reduce the formation of insoluble TTR-derived material when seeded with ATTR *ex vivo* fibrils.

fibril formation by quantifying the protein content in the insoluble fraction after 24 h of incubation at 37 °C (Fig. 5*a*) and immunodot blot of the insoluble fraction (Fig. 5*b*). The presence or absence of protein aggregates was confirmed by EM (Fig. 5*c*). A scrambled version of our peptide inhibitor, *H1*, was included as a negative control. We found that the efficacy of TabFH2 was dose-dependent, and although its efficiency differs from sample to sample, for every sample full inhibition was observed at the highest concentration analyzed (Fig. 5, *a–c*). This variability did not correlate with mutational background of the *ex vivo* seeds. In contrast, we found an inverse relationship between TabFH2 effectiveness and the amount of TTR C-term fragments in the *ex vivo* resuspension (Fig. 5*d*). The content of fragmented TTR, present in type A amyloidosis, was quantified from two independent Western blots using an antibody that specifically recognizes TTR C-terminal fragments, as we previously described (3). Pearson's correlation coefficient between amyloid seeding in the presence of 180 μM TabFH2 and TTR fragment content was 0.90 (R-square = 0.80) indicating a positive correlation. In addition, we evaluated the effect of inhibitors on the seeds extracted from an ATTR-V30M patient (Fig. 5, *e* and *f*). As mentioned above, ATTR-V30M is the most common form of hereditary ATTR that manifests progressive polyneuropathy and autonomic symptoms (12). We observed a similar pattern: TabFH2 offers an inhibitory effect, whereas tafamidis and diflunisal show limited inhibition of seeding (Fig. 5, *e* and *f*).

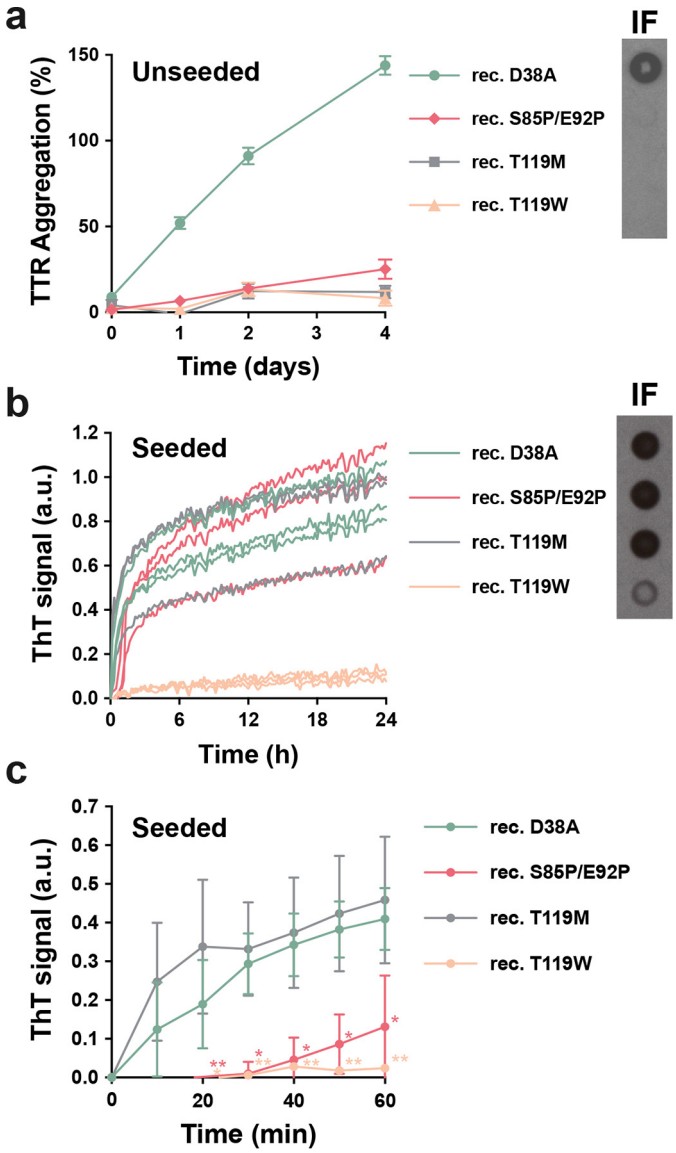

Figure 3. Mutational tetramer stabilization does not halt amyloid seeding. *a,* aggregation assay of 1 mg/ml of nonaggregating recombinant TTR mutants in the absence of seeds at pH 4.3, followed by absorbance at 400 nm. The assay shows that the T119M and other nonaggregating variants do not aggregate at pH 4.3 if unseeded. Aggregation of WT transthyretin was considered as 100%. *Right inset*, anti-TTR dot blot of insoluble fractions collected by centrifugation after 4 days of incubation. $n = 3$. *Error bars*, S.D. *b,* amyloid seeding assay of nonaggregating mutants in the presence of ATTR-D38A *ex vivo* seeds, monitored by ThT fluorescence at pH 4.3. Notice that T119M does aggregate when seeded. *Right inset*, anti-TTR dot-blot of insoluble fractions collected after 24 h of incubation. All replicates are shown, $n = 3$. *a.u.*, arbitrary units. *c,* short-time view of the lag phase of the amyloid seeding assay shown in *b*. $n = 3$. *Error bars*, S.D. *, $p \leq 0.05$ and **, $p \leq 0.005$.

TabFH2 inhibitory activity is tissue independent

We extracted *ex vivo* seeds from small quantities of two additional tissue types to evaluate tissue specificity of TabFH2. We extracted ATTR seeds from five samples of adipose tissue collected in fat pad biopsies, including one case of WT ATTR and four cases of hereditary ATTR, and two samples of labial salivary glands from two ATTR-V30M patients (Table 1). Because biopsy specimens were considerably smaller than the cardiac tissue samples (30–150 mg *versus* 1–5 g), we downsized the amyloid extraction protocol accordingly. Otherwise, the proce-

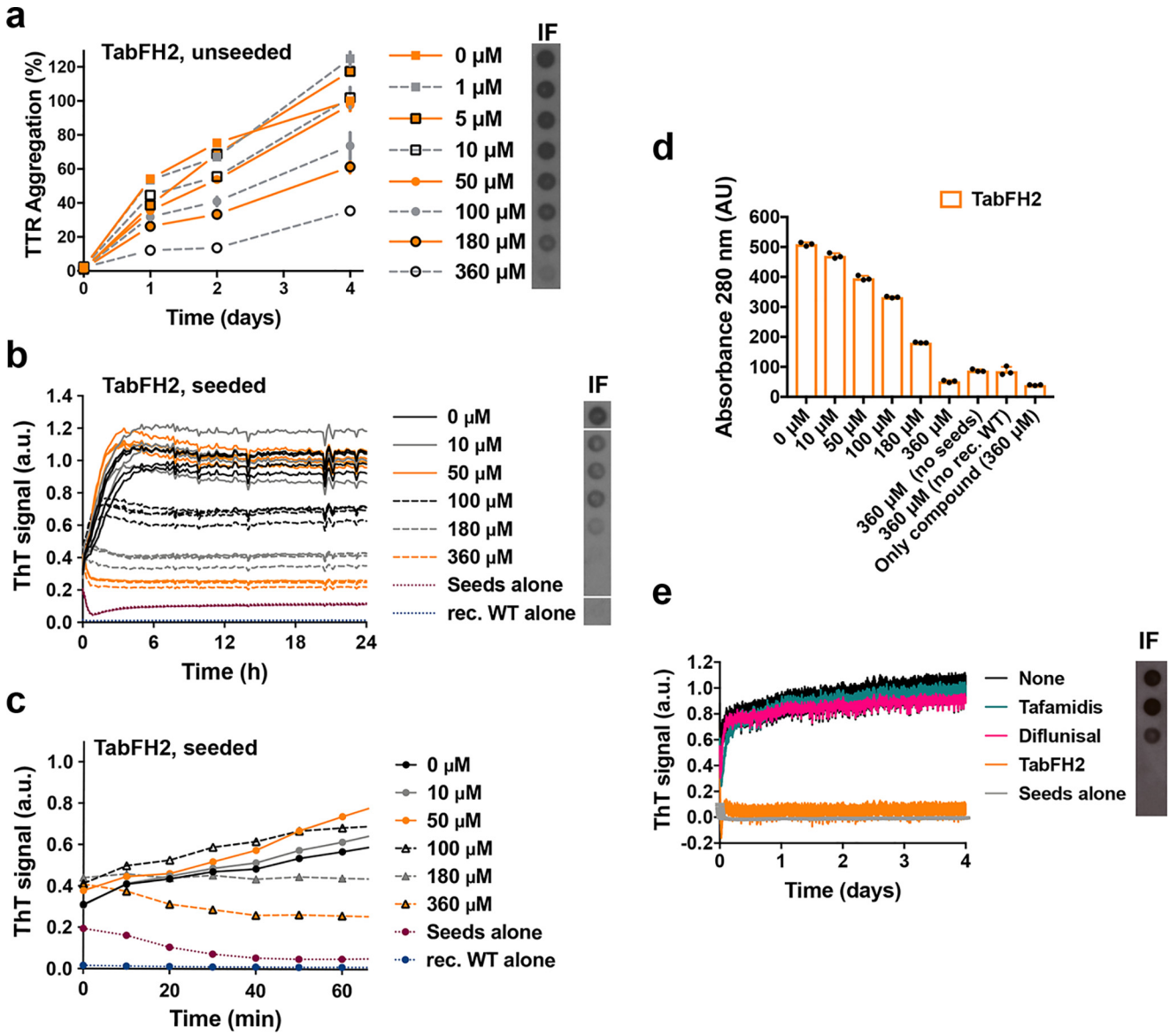

Figure 4. The anti-amyloid peptide inhibitor TabFH2 inhibits TTR aggregation and amyloid seeding caused by ATTR *ex vivo* seeds extracted from ATTR-D38A cardiac tissue. *a*, inhibition of TTR aggregation by TabFH2 in the absence of seeds, measured by absorbance at 400 nm. Increasing amounts of TabFH2 were added to 1 mg/ml of recombinant WT TTR and the sample was incubated for 4 days at pH 4.3. Absorbance measured after 4 days of incubation in the absence of TabFH2 was considered 100% aggregation because no soluble TTR was detected. $n = 3$. *Error bars*, S.D. *Right inset*, anti-TTR dot-blot of insoluble fractions (*IF*) collected by centrifugation after 4 days of incubation. *b*, inhibition of amyloid seeding by TabFH2 at pH 4.3, monitored by ThT fluorescence. Increasing amounts of TabFH2 were added to 0.5 mg/ml of recombinant WT TTR and 30 ng/μl of ATTR-D38A seeds. All replicates are shown, $n = 4$. *a.u.*, arbitrary units. *Inset*, anti-TTR dot-blot of insoluble fractions collected by centrifugation after 24 h of incubation. All samples were spotted onto the same nitrocellulose membrane and subjected to the same procedure; splicing was needed for presentation purposes. *c*, short-time view of the lag phase of the assay shown in *b*. $n = 4$. *Error bars*, S.D. *d*, protein content quantification of the insoluble fractions collected from *b*, measured by 280 nm absorbance. *AU*, absorbance units. Notice that the reduction of ThT fluorescence observed in *b* correlates with the decrease of total protein and TTR content in the insoluble fractions, shown in *c* and the *right inset* of *b*, respectively. *e*, comparison of inhibition of amyloid seeding by tafamidis, diflunisal, and TabFH2 when incubated for 4 days, measured by ThT fluorescence. 360 μM inhibitor was added to 0.5 mg/ml of recombinant WT TTR and 30 ng/μl of ATTR-D38A seeds. $n = 3$. *Error bars*, S.D. *Inset*, anti-TTR dot-blot of insoluble fractions collected by centrifugation after 4 days of incubation.

dure remained as previously described (3). The extraction from fat pad biopsies produced a very limited amount of insoluble material. We were therefore forced to reduce the amount of *ex vivo* seeds used in amyloid seeding assays to 5 ng/μl. Due to the formation of structurally different species or perhaps a result of the small amount of seeds that were added to the assay, the ThT signal was insufficient to draw any conclusion. For this reason, we opted to follow amyloid seeding by image-based computational quantification of protein aggregates after 24 h of incubation (Fig. 6). We collected images of the bottom of 96-well plates by optical microscopy using the Celigo S Imaging system. The images showed the formation of UV-positive aggregates in those samples that contained *ex vivo* seeds and no apparent aggregation in the control sample (Fig. 6*a*). The inhibitory effect of TabFH2 was confirmed by a significant reduction of amyloid conversion at 180 μM (Fig. 6*b*). Together, our results indicate that TabFH2 efficiently inhibits amyloid seeding caused by WT and mutant *ex vivo* seeds in a tissue-independent manner, for the range of tissues we studied.

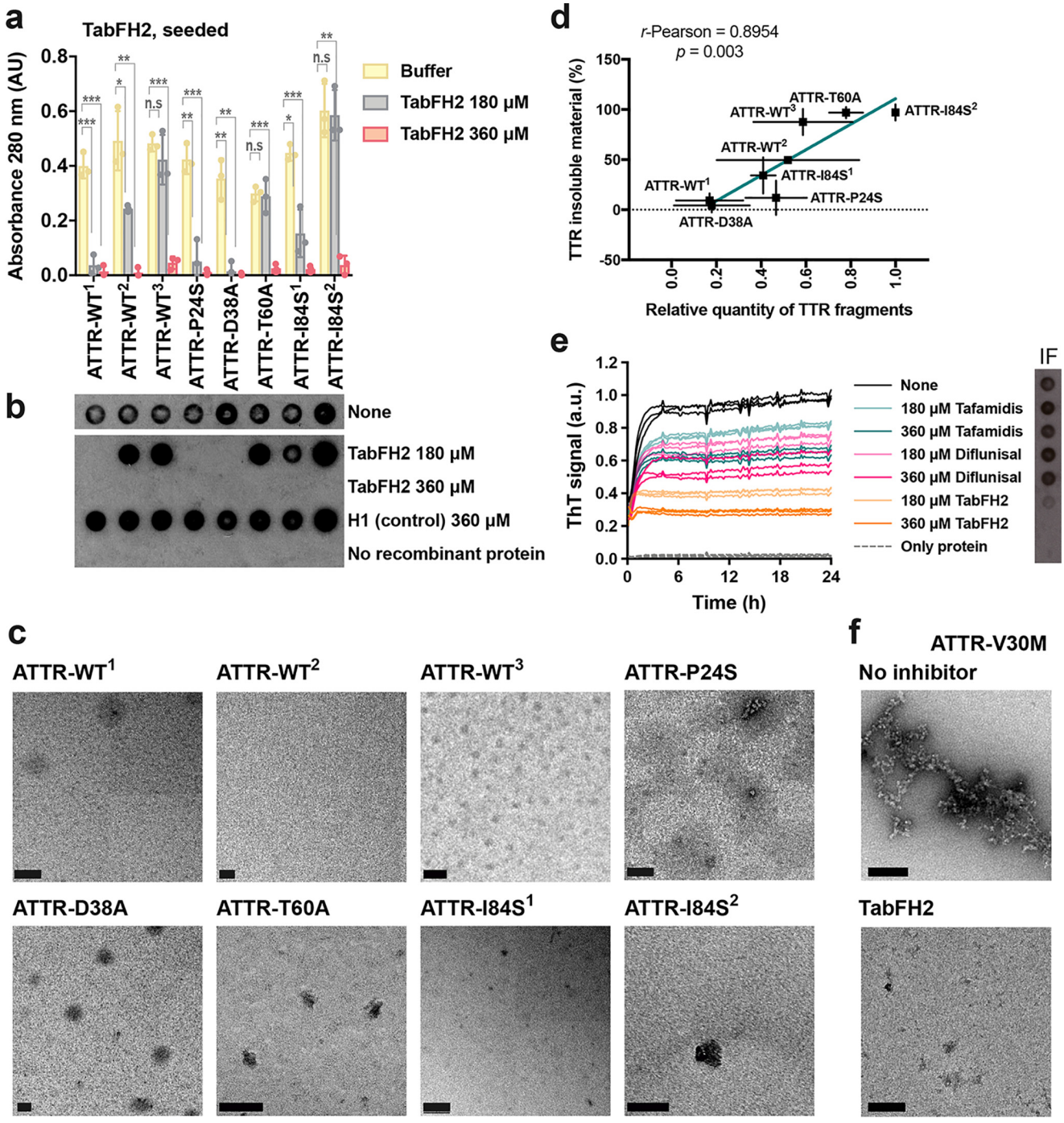

Figure 5. TabFH2 inhibits amyloid seeding caused by *ex vivo* ATTR seeds extracted from all cardiac extracts studied. *a,* inhibition of amyloid seeding by TabFH2 in the presence of cardiac *ex vivo* seeds, measured by protein content quantification of insoluble fractions. 30 ng/μl of *ex vivo* seeds extracted from the hearts of eight ATTR patients were added to 0.5 mg/ml of recombinant WT transthyretin in the presence of 0, 180, or 360 μM TabFH2. The insoluble fractions were collected by centrifugation after 24 h of incubation. The insoluble protein content was measured by absorbance at 280 nm. The results show that full inhibition of amyloid seeding by TabFH2 is achieved at the highest concentration for every ATTR *ex vivo* sample. $n = 3$. *Error bars*, S.D. *, $p \leq 0.05$; **, $p \leq 0.005$; ***, $p \leq 0.0005$. *b,* TTR immunodot blot of insoluble fractions collected by centrifugation from the assay shown in *a*, with consistent results. The experiment shown in *a* and *b* was performed in combination with the assay shown in Fig. 2; therefore the control samples without seeds are the same. All samples, including those from Fig. 2, were spotted onto the same nitrocellulose membrane and subjected to the same procedure; splicing was needed for presentation purposes. *c,* electron micrographs of the samples containing 360 μM TabFH2 collected from *a*. These are uncorrected images generated directly from a Gatan 2kX2k CCD camera. *Scale bar*, 200 nm. *d,* correlation between amyloid seeding capacity in the presence of 180 μM TabFH2, and relative quantity of truncated TTR of *ex vivo* ATTR seeds. Notice that the presence of truncated TTR facilitates seeding. Truncated TTR content was quantified by ImageJ from two independent Western blots. Lineal regression and Pearson *r* were obtained by OriginLab. *e,* comparison of inhibition of ATTR-V30M amyloid seeding by tafamidis, diflunisal, and TabFH2, measured by ThT fluorescence. 180 or 360 μM inhibitor was added to 0.5 mg/ml of recombinant WT TTR and 30 ng/μl of ATTR-V30M seeds. All replicates are shown, $n = 4$. *a.u.*, arbitrary units. *Inset*, anti-TTR dot-blot of insoluble fractions collected by centrifugation after 24 h of incubation. *f*, electron micrographs of the samples collected from *e*.

TABLE 1
Tissue specimens used for amyloid extraction
A total of 8 cardiac, 5 adipose, and 2 glandular specimens were included in this study. Patients presenting the same TTR variant are indicated by superscripts.

Cardiac Tissue Specimens

Mutation	Origin	f/m	Age	Neuropathy signs	Weight (g)
ATTR-WT[1]	Post mortem	m	84	No	1.6
ATTR-WT[2]	Post mortem	m	70	No, but amyloid found at autopsy	2.8
ATTR-WT[3]	Transplant	m	78	No	3.4
ATTR-P24S	Transplant	m	65	No	2.3
ATTR-V30M	Post mortem	m	60	Yes	2.5
ATTR-D38A	Transplant	f	59	Unknown	4.5
ATTR-T60A	Post mortem	m	57	Moderate	2.2
ATTR-I84S[1]	Post mortem	f	56	No, but amyloid found at autopsy	2.7
ATTR-I84S[2]	Post mortem	m	53	Mild	1.1

Fat biopsy specimens

Mutation	Congo Red (0-4)	f/m	Age	Wet fat (mg)	ng TTR/ mg fat
ATTR-WT	3	m	73	58.9	51.8
ATTR-V30M	4	f	47	78.5	618.7
ATTR-A45G	4	m	77	91.8	657.7
ATTR-G47E	4	m	35	31.3	433.3
ATTR-V122del	3	m	59	17.7	84.2

Labial salivary gland biopsy specimens

Mutation	f/m	Age
ATTR-V30M[1]	Unknown	Unknown
ATTR-V30M[2]	Unknown	Unknown

TabFH2 inhibits amyloid seeding by binding to ATTR fibrils

Our peptide inhibitors were originally designed and optimized to cap the tip of TTR fibrils by binding β-strands F and H (3, 10). To validate our design, we next assessed binding of TabFH2 to ATTR seeds (Fig. 7). We first immobilized 5 μg of ATTR-D38A seeds on each of eight anti-TTR pre-coated wells. Binding of ATTR seeds to the bottom of the wells was confirmed later by BCA protein assay of unbound material. We then added increasing amounts of TabFH2 (0–500 μM) to pretreated wells. After 2 h of incubation, we analyzed the remaining amount of TabFH2 in the sample by HPLC. Anti-TTR precoated wells treated with buffer, but not seeds, were used as negative control to detect unspecific binding of TabFH2 to the well. Whereas the majority of TabFH2 remained in the sample after incubation in negative control wells, most of TabFH2 was absent when wells were pretreated with ATTR seeds (Fig. 7*d*). Our results indicate that the mechanism of action of our peptide inhibitors involves binding to ATTR fibrils.

Discussion

Extensive studies by others have established that ligands such as tafamidis and diflunisal bind within TTR and stabilize its tetrameric structure, diminishing its rate of dissociation and hence its conversion to amyloid fibrils (5–7). The data of Fig. 1, *a* and *b,* confirm the stabilization of TTR by tafamidis and diflunisal. Indeed tafamidis has been prescribed for the treatment of neuropathic ATTR-V30M and ameliorates disease progression when administered at disease stage I (16–19). Diflunisal has shown positive neurological effects in ATTR patients at different stages (9, 20). Despite the stabilization, our results show that disease-related seeds convert WT TTR into amyloid fibrils in the presence of these ligands at concentrations that fully inhibit aggregation of recombinant transthyretin in the absence of seeds (Figs. 1 and 2) (21, 22). Thus our results offer a plausible explanation for the reported limited efficacy of tafamidis over the long term, when administered at late stages, or in patients with severe cardiac involvement (8, 23, 24). That

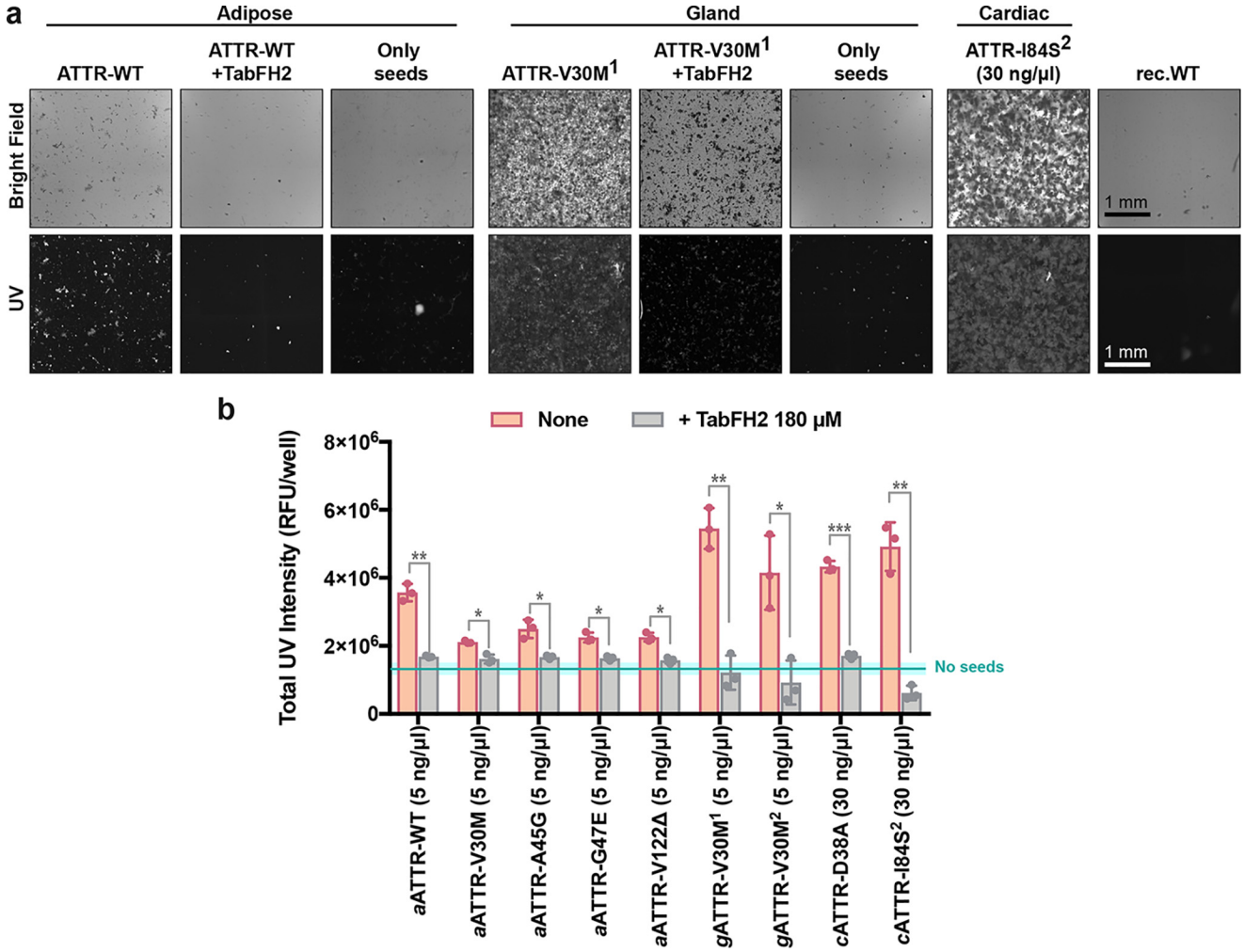

Figure 6. Inhibition of amyloid seeding caused by *ex vivo* ATTR seeds extracted from human fat pad and salivary gland biopsies. *a,* representative optical micrographs of aggregates of recombinant WT TTR formed after 24 h of incubation with 5 ng/μl of fat-extracted ATTR-WT or gland-extracted ATTR-V30M[1] *ex vivo* seeds, as visualized on a Celigo S Imaging system under bright field and UV channels. Images are composites generated by the Celigo S Imaging system. *Scale bar*, 1 mm; all images have the same scale. Note that the addition of TabFH2 results in the reduction of UV-positive aggregates. Three control samples are included: samples containing only seeds, recombinant WT TTR aggregates formed after incubation with 30 ng/μl of cardiac ATTR-D38A seeds, and recombinant WT TTR in the absence of seeds (*rec.WT*). *b,* UV intensity-based quantification of protein aggregates after 24 h of incubation of recombinant WT TTR with ATTR *ex vivo* seeds extracted from various adipose tissue and salivary gland samples (labeled with *italic a* and *g,* respectively). The presence of 180 μM TabFH2 resulted in the inhibition of amyloid seeding for all studied samples. *Cyan line* and *rectangle* represent the UV intensity mean ± S.D. range in the absence of seeds, respectively. $n = 3$. *Error bars*, S.D. *, $p \leq 0.05$; **, $p \leq 0.005$; ***, $p \leq 0.0005$, for the comparison between samples with and without TabFH2.

is, stabilization of tetrameric TTR may be insufficient in situations in which seeded polymerization dominates rather than *de novo* nucleation of TTR seeds.

Genetically stabilized TTR fails to inhibit seeded fibril formation. The genetic variant T119M of TTR and its capacity to delay fibril formation was originally found in an ATTR-V30M family because of its protective effects; this variant remains soluble at pH 4.3 for weeks, if not months (Fig. 3*a*) (10, 14, 25). However, in our experiments, this stabilized variant does not halt conversion to amyloid in the presence of *ex vivo* seeds (Fig. 3, *b* and *c*). These findings may explain why heterozygous individuals carrying both the hereditary amyloidogenic *ttr*-V30M allele and the stabilizing *ttr*-T119M allele in time-developed ATTR (14, 15). In ATTR-V30M/T119M patients, we hypothesize that the mutation T119M may delay the progression of ATTR by reducing *de novo* nucleation.

The limited effect of TTR tetramer stabilization in our experiments does not contradict the well-established mechanism of *de novo* formation of TTR amyloid (26). In our previous study, we showed that the conversion of TTR to amyloid fibrils requires the dissociation of tetramers and partial unfolding of monomers, which takes place as the pH is lowered to 4.3, exposing the adhesive amyloidogenic segments. The monomeric variant MTTR, which exposes these segments, can be seeded at physiological pH (3). TTR dissociation and subsequent seeded or unseeded polymerization may be triggered by a variety of factors, such as protease cleavage or local pH disturbances. In our assays, amyloid seeding is also performed at low pH to weaken the quaternary structure and to lead to tetramer dissociation. Under acidic conditions, the addition of seeds to recombinant TTR causes acceleration of fibril formation through seeded polymerization. We reason that this seeded polymerization results in fibrils that are resilient to disassembly, thereby making the pathway irreversible. Because the interaction of TTR with the tetramer stabilizers is not irreversible, the presence of seeds will eventually reduce

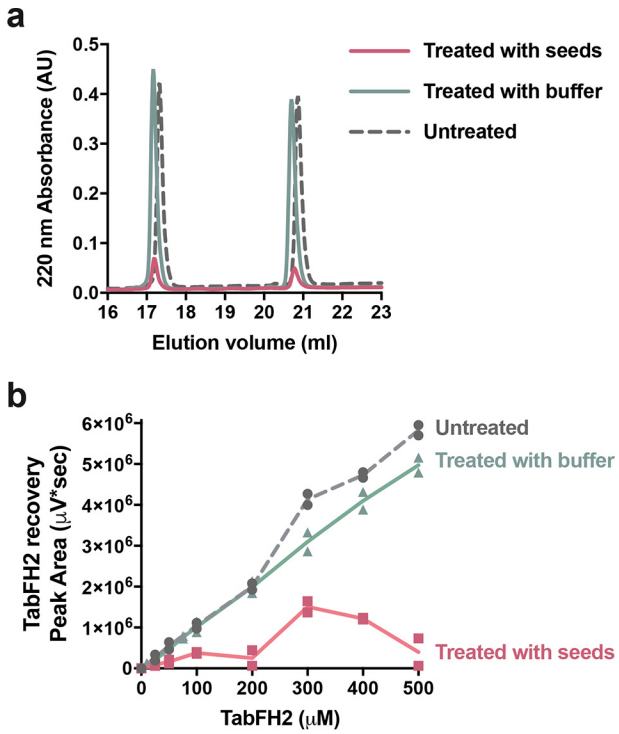

Figure 7. TabFH2 binds ATTR *ex vivo* seeds. Increasing amounts of TabFH2 were added to independent wells pretreated with ATTR seeds (*treated with seeds*) or buffer (*treated with buffer*), and unbound TabFH2 was detected by reverse-phase chromatography. TabFH2 samples before treatment were included in the analysis (*untreated*). *a,* representative HPLC elution profile for a TabFH2 concentration of 500 μM showing two peaks: TabH2 eluting at ~17 ml and TabF2 eluting at ~21 ml. *b,* analysis of TabFH2 recovery at all concentrations, measured as peak area integrated from HPLC elution profiles. The graph shows that the recovery of both TabF2 and TabH2 when wells were pretreated with ATTR seeds was significantly lower than when pretreated with buffer.

both monomeric and tetrameric pools while generating irreversible amyloid fibrils.

Capping of TTR amyloid fibrils by designed peptides is an effective approach to inhibit TTR fibril seeding. Our results show that in cases for which stabilization of tetrameric TTR by ligands may not be fully effective in halting fibril formation (Figs. 1 and 2), capping of TTR fibrils by designed blockers of fibril elongation is effective (Figs. 4–6). This may be of special importance for cardiac ATTR patients, who are often diagnosed when manifesting advanced TTR deposition and have limited treatment options. In the conditions of our experiments, TabFH2 blockers are effective in halting fibril formation caused by WT ATTR seeds and also by seeds of at least six disease-related variants extracted from *ex vivo* cardiac specimens (Fig. 5). Overall, we find that the inhibition of amyloid seeding by peptide inhibitors is an effective strategy independent of pathological variant or tissue (Figs. 5 and 6).

Structure-based inhibition of amyloid aggregation by peptides is an emergent strategy that has shown promising results. Our structure-based strategy has generated peptide inhibitors of Tau fibril formation that is associated with Alzheimer's disease (27, 28), SEVI amyloid aggregation that enhances HIV transmission (28), and p53 aggregation associated with certain types of ovarian cancer (29). In our previous work on inhibition of TTR, we generated TTR peptide inhibitors that block both protein aggregation and amyloid seeding catalyzed by *ex vivo* ATTR fibrils (3, 10). Moreover, diseased flies showed motor improvement and a reduction of TTR deposition after treatment with our peptide inhibitors (30). In this study, we expand the evaluation of peptide inhibitors to question their inhibitory capacity compared with two tetramer stabilizers and mutagenesis-based stabilization. Fig. 8 depicts how we envision the mechanism by which TabFH2 and tetramer stabilizers inhibit amyloid seeding and aggregation, respectively. The peptide inhibitor TabFH2 was previously designed to bind strands F and H, the two amyloid driving segments of TTR, thereby halting self-association and further polymerization (3, 10). Other groups have expanded on our work on the inhibition of TTR aggregation by impeding self-association of the amyloid-driving strands F and H of TTR using monoclonal antibodies (31, 32). Our results indicate that the inhibition of amyloid seeding by peptide inhibitors may represent a potential therapeutic strategy for ATTR when tetramer stabilization is not sufficient to halt disease progression.

Experimental procedures

Antibodies

The antibodies used in this study include rabbit anti-human transthyretin polyclonal antibody (DAKO, Agilent Technologies; immunodot blots and Western blots, 1:10,000) and horseradish peroxidase-conjugated goat anti-rabbit IgG antibody (Thermo Fisher Scientific, immune dot blots and Western blots, 1:5,000). Anti-truncated TTR was generously provided by Gunilla Westermark (labeled as 1898, Western blots, 1:5,000).

Patients and tissue materials

Twenty-one ATTR patients carrying WT (n = 4) or TTR mutations (n = 17) were included in this study (refer to Table 1 for full details). Cardiac tissue specimens were obtained from several laboratories from explanted hearts or by autopsy. Adipose tissues were obtained from needle biopsy procedures performed at the University Medical Centre Groningen. Salivary gland tissues were obtained from surgical biopsy procedures performed at the Hospital Santo António in Porto. The UCLA Office of the Human Research Protection Program granted exemption from IRB review because all specimens were anonymized. These studies abide by the Declaration of Helsinki principles.

Extraction of amyloid fibrils from tissue samples

Amyloid fibrils were extracted from fresh-frozen human tissue following a previously described protocol (3). In short, thawed tissue sample, resuspended in 10 ml of 0.15 M NaCl, was minced with a motorized homogenizer and pelleted by centrifugation at 15,000 rpm for 30 min. The pellet was subject to further cycles of resuspension, homogenization, and centrifugation first with 0.15 M NaCl solution 7 times, followed by distilled water 3 times. Because there was less starting material for both adipose tissue and salivary gland specimens, the extraction protocol was downsized in volume accordingly. The final pellet was lyophilized, and amyloid content of the extracts was confirmed by EM. TTR content of the samples was analyzed by anti-TTR Western blotting.

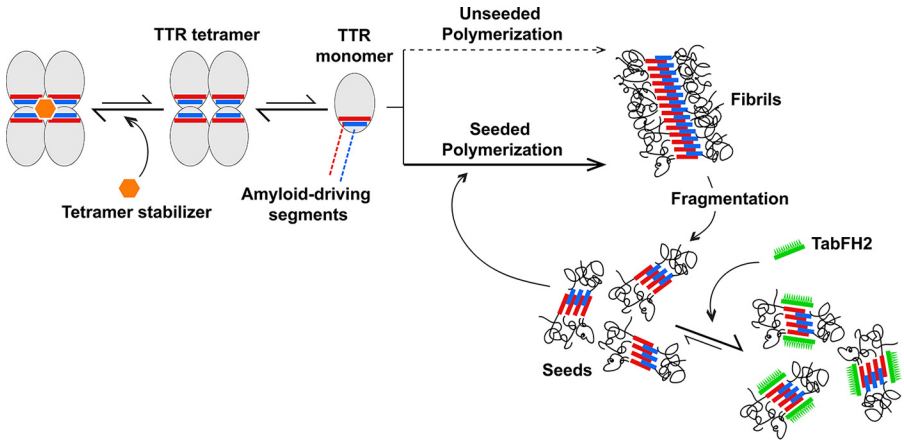

Figure 8. Model of TTR amyloid seeding and its inhibition. TTR dissociation provides monomers that are susceptible to nucleation and fibril formation through self-association of amyloid-driving segments. TTR ligands such as tafamidis or diflunisal stabilize the tetrameric form, decelerating tetramer dissociation and unseeded polymerization. After fragmentation of fibrils, small fragments may serve as seeds that template fast polymerization. The peptide inhibitor TabFH2 does not affect tetramer stability. Instead, TabFH2 binds to seeds, hindering self-recognition and seeding. Both strategies seem synergistic and could potentially be used in combination.

Purification of recombinant TTR

Recombinant transthyretin was prepared as described previously (10). To summarize, *Escherichia coli* cells (Millipore Rosetta DE3 pLysS Competent Cells) were transformed with a pET24(+) vector carrying the sequence for either WT or a mutant of transthyretin. The expressed recombinant protein was harvested and purified by nickel affinity chromatography with a HisTrap column (GE Healthcare). The appropriate fractions were pooled and further purified by size exclusion on a Superdex 75 gel filtration column (GE Healthcare). Recombinant transthyretin was stored in 10 mM sodium phosphate, pH 7.5, 100 mM KCl, and 1 mM EDTA at −20 °C.

Western blotting of tissue extracts

TTR content of tissue extracts was confirmed by Western blotting as described previously (3). To summarize, equal amounts of total protein were loaded on a 4–12% NuPAGE BisTris gel (ThermoFisher Scientific) and separated by gel electrophoresis in denaturing conditions. TTR was detected after transfer to a nitrocellulose membrane with polyclonal anti-human transthyretin antibody or anti-truncated TTR antibody and horseradish peroxidase-conjugated secondary goat anti-rabbit IgG. SuperSignal™ West Pico Chemiluminescent Substrate (ThermoFisher Scientific) was used according to the manufacturer's instructions to visualize TTR content. Truncated TTR content of cardiac seeds was quantified by ImageJ using two independent Western blots.

Congo red staining and TTR content quantification of adipose tissue

Abdominal fat smears were made as previously described (33). Slides were stained with alkaline Congo red (34) and apple-green birefringence under polarized light were semi-quantitatively scored as follows: 0 (negative), 1 (min, <1% surface area), 2 (little, between 1 and 10%), 3 (moderate, between 10 and 60%), and 4 (abundant, >60%). The remaining abdominal fat tissue was weighed and washed. Proteins were resuspended with a Tris-guanidinium hydrochloride solution, and TTR content was measured by ELISA. Briefly, microtiter plates were coated overnight with the extracts and human native TTR protein (Abcam, Cambridge, UK), which served as control, in several dilutions. Detection was done by using rabbit anti-human TTR polyclonal antibodies (DAKO, Agilent Technologies) followed by horseradish peroxidase-conjugated goat anti-rabbit IgG antibody (DAKO, Agilent Technologies) and visualized by a color reaction with TMB ELISA substrate. Plates were scanned at 450 nm after stopping the reaction with sulfuric acid.

Peptides

Peptides were synthesized at >97% purity by GL Biochem (Shanghai) Ltd. (Shanghai, China). Purity and molecular weight were confirmed by MALDI-TOF and reversed phase HPLC. TabFH2 is an equimolar mixture of RRRRHVAHPFV(*N*-methyl)EFTE and RRRRSYVTNPTSY(*N*-methyl)AVT, as previously described (3). Peptides were dissolved in 0.22 μm of filtered water to 5 mM stock solution. These working solutions were further diluted prior to use to the final concentration.

Non-seeded TTR aggregation

TTR aggregation assays were done as previously described (10). Briefly, 1 mg/ml of TTR sample in 100 mM sodium acetate, pH 4.3, 100 mM KCl, 1 mM EDTA was incubated in the presence or absence of inhibitor, diflunisal, tafamidis, or TabFH2, at 37 °C for 4 days. TTR aggregation was followed by measuring sample turbidity at 400 nm and by anti-TTR immunodot blot of the insoluble fraction.

TTR amyloid-seeding assay

Extracted tissue samples were used to seed the formation of transthyretin amyloid fibrils following a protocol described previously (3). In short, extracts were washed twice in 1% SDS and twice in 10 mM sodium phosphate, pH 7.5, 100 mM KCl, 1 mM EDTA. Next, the extracts were sonicated at minimum intensity with 5-s pulses for a total of 10 min. Protein concentration of the samples was determined by Pierce™ BCA Protein Assay Kit (ThermoFisher Scientific). Seeding reactions contained 0.5 mg/ml of recombinant protein, 30 ng/μl of car-

diac extract or in the case of adipose and gland extracts 5 ng/μl, 5 μM thioflavin T, 100 mM sodium acetate, pH 4.3, 100 mM KCl, and 1 mM EDTA. The inhibitors mentioned, diflunisal, tafamidis, and TabFH2, were added at concentrations described in the figure legends. Thioflavin T fluorescence emission was measured at 482 nm with excitation at 440 nm in a FLUOstar Omega (BMG LabTech) plate reader. Plates were incubated at 37 °C for 24 h with orbital shaking at 700 rpm between measurement points. In all assays, measurements were normalized by subtracting the initial ThT measurement and considering the maximum signal as 100%. Protein aggregates were visualized by both bright field and UV and TTR aggregation was quantified using a Celigo S Imaging system. The insoluble fraction was obtained by centrifuging the sample and resuspending the pellet in guanidinium hydrochloride. Protein content of the pellet was determined by measuring absorbance at 280 nm.

Anti-TTR immunodot blot

TTR aggregation was confirmed by immunodot blot as mentioned previously (10). After obtaining the insoluble fraction by centrifugation and resuspension in guanidinium hydrochloride, 15 μl of sample was dotted onto a nitrocellulose membrane (0.2 μm, Bio-Rad). TTR content was visualized using polyclonal rabbit anti-human transthyretin (DAKO), horseradish peroxidase-conjugated goat anti-rabbit IgG antibody (ThermoFisher Scientific), and SuperSignal™ West Pico Chemiluminescent Substrate (ThermoFisher Scientific).

Transmission electron microscopy

Amyloid content of tissue extracts and inhibition of fibril formation was confirmed by transmission EM. 5 μl of sample was applied to a glow-discharged carbon-coated EM grid (CF150-Cu, Electron Microscopy Sciences) for 4 min. After three quick rinses in distilled water, grids were stained with 2% uranyl acetate for 2 min. Samples were visualized using a T12 Quick CryoEM and CryoET (FEI) transmission electron microscope using an acceleration voltage of 120 kV equipped with a Gatan 2,048 × 2,048 CCD camera.

Detection of TabFH2 binding to ATTR seeds

TabFH2 binding to ATTR seeds was analyzed by HPLC. First, ATTR-D38A fibrils were immobilized on anti-TTR precoated well plates (Prealbumin ELISA kit, Abcam) as follows. 50-ml samples containing 0.1 mg/ml of ATTR seeds were added on each well. Control wells were equally treated with buffer (10 mM sodium acetate, pH 7.5, 100 mM KCl, 1 mM EDTA). After 1-h incubation at room temperature, samples were then removed and wells were washed twice with buffer. Immobilization of the total amount of fibrils was confirmed by BCA protein assay of the remaining sample. 50-ml samples that contained increasing concentrations of TabFH2 (0–500 mM) were added to independent wells pretreated with ATTR seeds or buffer. After an incubation of 2 h at room temperature, samples were transferred to new tubes and snap frozen until further analysis. Unbound TabFH2 was detected by chromatography after 0.10 nm filtration, on a Waters 1525 HPLC System (SpectraLab), with a Proto 300 C18 5-mm 250 × 4.6-mm analytical reverse phase column (Higgins Analytical); flow rate = 1.0 ml/min; solvents: A = 0.1% TFA in water, and B = 0.1% TFA in acetonitrile. The column was equilibrated with 10% B for 5 min, followed by a gradient from 10 to 60% B in 30 min, and a 2-min wash at 95% B. TabFH2 eluted in two peaks after ~17 and 20 min from the start. Peaks were integrated by Breeze2 software and Prism was used for graphing.

Author contributions—L. S. and D. S. E. conceptualization; L. S., T. C., J. B., and M. D. B. resources; L. S. and K. C. data curation; L. S., K. C., and D. S. E. formal analysis; L. S. and D. S. E. supervision; L. S. and D. S. E. funding acquisition; L. S. and K. C. validation; L. S., B. A. N., K. C., Y. W., A. O., J. H. L., and J. B. investigation; L. S. visualization; L. S. methodology; L. S. writing-original draft; L. S. project administration; L. S., K. C., and D. S. E. writing-review and editing; K. C. software.

Acknowledgments—We thank Dr. Jeffery Kelly for a gift of tafamidis and discussions, Drs. Joel Buxbaum, Michael Sawaya, and Duilio Cascio for helpful discussion, and the patients who generously donated tissues.

References

1. Pinney, J. H., Whelan, C. J., Petrie, A., Dungu, J., Banypersad, S. M., Sattianayagam, P., Wechalekar, A., Gibbs, S. D., Venner, C. P., Wassef, N., McCarthy, C. A., Gilbertson, J. A., Rowczenio, D., Hawkins, P. N., Gillmore, J. D., and Lachmann, H. J. (2013) Senile systemic amyloidosis: clinical features at presentation and outcome. *J. Am. Heart Assoc.* **2,** e000098 Medline
2. Galant, N. J., Westermark, P., Higaki, J. N., and Chakrabartty, A. (2017) Transthyretin amyloidosis: an under-recognized neuropathy and cardiomyopathy. *Clin. Sci. (Lond)* **131,** 395–409 CrossRef Medline
3. Saelices, L., Chung, K., Lee, J. H., Cohn, W., Whitelegge, J. P., Benson, M. D., and Eisenberg, D. S. (2018) Amyloid seeding of transthyretin by *ex vivo* cardiac fibrils and its inhibition. *Proc. Natl. Acad. Sci. U.S.A.* **115,** 6741–6750 CrossRef Medline
4. Foss, T. R., Wiseman, R. L., and Kelly, J. W. (2005) The pathway by which the tetrameric protein transthyretin dissociates. *Biochemistry* **44,** 15525–15533 CrossRef Medline
5. Hammarström, P., Wiseman, R. L., Powers, E. T., and Kelly, J. W. (2003) Prevention of transthyretin amyloid disease by changing protein misfolding energetics. *Science* **299,** 713–716 CrossRef Medline
6. Miroy, G. J., Lai, Z., Lashuel, H. A., Peterson, S. A., Strang, C., and Kelly, J. W. (1996) Inhibiting transthyretin amyloid fibril formation via protein stabilization. *Proc. Natl. Acad. Sci. U.S.A.* **93,** 15051–15056 CrossRef Medline
7. Castaño, A., Helmke, S., Alvarez, J., Delisle, S., and Maurer, M. S. (2012) Diflunisal for ATTR cardiac amyloidosis. *Congest. Heart Fail.* **18,** 315–319 CrossRef Medline
8. Planté-Bordeneuve, V., Gorram, F., Salhi, H., Nordine, T., Ayache, S. S., Le Corvoisier, P., Azoulay, D., Feray, C., Damy, T., and Lefaucheur, J. P. (2017) Long-term treatment of transthyretin familial amyloid polyneuropathy with tafamidis: a clinical and neurophysiological study. *J. Neurol.* **264,** 268–276 CrossRef Medline
9. Sekijima, Y., Tojo, K., Morita, H., Koyama, J., and Ikeda, S. (2015) Safety and efficacy of long-term diflunisal administration in hereditary transthyretin (ATTR) amyloidosis. *Amyloid* **22,** 79–83 CrossRef Medline
10. Saelices, L., Johnson, L. M., Liang, W. Y., Sawaya, M. R., Cascio, D., Ruchala, P., Whitelegge, J., Jiang, L., Riek, R., and Eisenberg, D. S. (2015) Uncovering the mechanism of aggregation of human transthyretin. *J. Biol. Chem.* **290,** 28932–28943 CrossRef Medline
11. Benson, M. D. (2013) Liver transplantation and transthyretin amyloidosis. *Muscle Nerve* **47,** 157–162 CrossRef Medline
12. Yazaki, M., Tokuda, T., Nakamura, A., Higashikata, T., Koyama, J., Higuchi, K., Harihara, Y., Baba, S., Kametani, F., and Ikeda, S. (2000) Cardiac

amyloid in patients with familial amyloid polyneuropathy consists of abundant wild-type transthyretin. *Biochem. Biophys. Res. Commun.* **274,** 702–706 CrossRef Medline

13. Bergström, J., Gustavsson, A., Hellman, U., Sletten, K., Murphy, C. L., Weiss, D. T., Solomon, A., Olofsson, B. O., and Westermark, P. (2005) Amyloid deposits in transthyretin-derived amyloidosis: cleaved transthyretin is associated with distinct amyloid morphology. *J. Pathol.* **206,** 224–232 CrossRef Medline
14. Coelho, T., Carvalho, M., Saraiva, M. J., Alves, I., Almeida, M. R., and Costa, P. P. (1993) A strikingly benign evolution of FAP in an individual found to be a compound heterozygote for two TTR mutations: TTR MET 30 and TTR MET 119. *J. Rheumatol.* **20,** 179
15. Coelho, T., Chorão, R., Sousa, A., Alves, I., Torres, M. F., and Saraiva, M. J. M. (1996) Compound heterozygotes of transthyretin Met30 and transthyretin Met119 are protected from the devastating effects of familial amyloid polyneuropathy. *Neuromusc. Disord.* **6,** S20 CrossRef
16. Waddington Cruz, M., and Benson, M. D. (2015) A review of tafamidis for the treatment of transthyretin-related amyloidosis. *Neurol. Ther.* **4,** 61–79 CrossRef Medline
17. Waddington Cruz, M., Amass, L., Keohane, D., Schwartz, J., Li, H., and Gundapaneni, B. (2016) Early intervention with tafamidis provides long-term (5.5-year) delay of neurologic progression in transthyretin hereditary amyloid polyneuropathy. *Amyloid* **23,** 178–183 CrossRef Medline
18. Coelho, T., Maia, L. F., Martins da Silva, A., Waddington Cruz, M., Planté-Bordeneuve, V., Lozeron, P., Suhr, O. B., Campistol, J. M., Conceição, I. M., Schmidt, H. H., Trigo, P., Kelly, J. W., Labaudinière, R., Chan, J., Packman, J., *et al.* (2012) Tafamidis for transthyretin familial amyloid polyneuropathy: a randomized, controlled trial. *Neurology* **79,** 785–792 CrossRef Medline
19. Obici, L., and Merlini, G. (2014) An overview of drugs currently under investigation for the treatment of transthyretin-related hereditary amyloidosis. *Expert Opin. Investig. Drugs* **23,** 1239–1251 CrossRef Medline
20. Berk, J. L., Suhr, O. B., Obici, L., Sekijima, Y., Zeldenrust, S. R., Yamashita, T., Heneghan, M. A., Gorevic, P. D., Litchy, W. J., Wiesman, J. F., Nordh, E., Corato, M., Lozza, A., Cortese, A., Robinson-Papp, J., *et al.* (2013) Repurposing diflunisal for familial amyloid polyneuropathy: a randomized clinical trial. *JAMA* **310,** 2658–2667 CrossRef Medline
21. Bulawa, C. E., Connelly, S., Devit, M., Wang, L., Weigel, C., Fleming, J. A., Packman, J., Powers, E. T., Wiseman, R. L., Foss, T. R., Wilson, I. A., Kelly, J. W., and Labaudinière, R. (2012) Tafamidis, a potent and selective transthyretin kinetic stabilizer that inhibits the amyloid cascade. *Proc. Natl. Acad. Sci. U.S.A.* **109,** 9629–9634 CrossRef Medline
22. Adamski-Werner, S. L., Palaninathan, S. K., Sacchettini, J. C., and Kelly, J. W. (2004) Diflunisal analogues stabilize the native state of transthyretin: potent inhibition of amyloidogenesis. *J. Med. Chem.* **47,** 355–374 CrossRef Medline
23. Lozeron, P., Théaudin, M., Mincheva, Z., Ducot, B., Lacroix, C., Adams, D., and French Network for FAP (CORNAMYL) (2013) Effect on disability and safety of Tafamidis in late onset of Met30 transthyretin familial amyloid polyneuropathy. *Eur. J. Neurol.* **20,** 1539–1545 CrossRef Medline
24. Fujita, T., Inomata, T., Kaida, T., Iida, Y., Ikeda, Y., Nabeta, T., Ishii, S., Maekawa, E., Naruke, T., Koitabashi, T., Kitamura, E., Sekijima, Y., and Ako, J. (2017) Tafamidis for the treatment of hereditary transthyretin amyloid cardiomyopathy: a case report. *Cardiology* **137,** 74–77 CrossRef Medline
25. McCutchen, S. L., Lai, Z., Miroy, G. J., Kelly, J. W., and Colón, W. (1995) Comparison of lethal and nonlethal transthyretin variants and their relationship to amyloid disease. *Biochemistry* **34,** 13527–13536 CrossRef Medline
26. Hurshman, A. R., White, J. T., Powers, E. T., and Kelly, J. W. (2004) Transthyretin aggregation under partially denaturing conditions is a downhill polymerization. *Biochemistry* **43,** 7365–7381 CrossRef Medline
27. Seidler, P. M., Boyer, D. R., Rodriguez, J. A., Sawaya, M. R., Cascio, D., Murray, K., Gonen, T., and Eisenberg, D. S. (2018) Structure-based inhibitors of tau aggregation. *Nat. Chem.* **10,** 170–176 CrossRef Medline
28. Sievers, S. A., Karanicolas, J., Chang, H. W., Zhao, A., Jiang, L., Zirafi, O., Stevens, J. T., Münch, J., Baker, D., and Eisenberg, D. (2011) Structure-based design of non-natural amino-acid inhibitors of amyloid fibril formation. *Nature* **475,** 96–100 CrossRef Medline
29. Soragni, A., Janzen, D. M., Johnson, L. M., Lindgren, A. G., Thai-Quynh Nguyen, A., Tiourin, E., Soriaga, A. B., Lu, J., Jiang, L., Faull, K. F., Pellegrini, M., Memarzadeh, S., and Eisenberg, D. S. (2016) A designed inhibitor of p53 aggregation rescues p53 tumor suppression in ovarian carcinomas. *Cancer Cell* **29,** 90–103 CrossRef Medline
30. Saelices, L., Pokrzywa, M., Pawelek, K., and Eisenberg, D. S. (2018) Assessment of the effects of transthyretin peptide inhibitors in *Drosophila* models of neuropathic ATTR. *Neurobiol. Dis.* **120,** 118–125 CrossRef Medline
31. Higaki, J. N., Chakrabartty, A., Galant, N. J., Hadley, K. C., Hammerson, B., Nijjar, T., Torres, R., Tapia, J. R., Salmans, J., Barbour, R., Tam, S. J., Flanagan, K., Zago, W., and Kinney, G. G. (2016) Novel conformation-specific monoclonal antibodies against amyloidogenic forms of transthyretin. *Amyloid* **23,** 86–97 CrossRef Medline
32. Hosoi, A., Su, Y., Torikai, M., Jono, H., Ishikawa, D., Soejima, K., Higuchi, H., Guo, J., Ueda, M., Suenaga, G., Motokawa, H., Ikeda, T., Senju, S., Nakashima, T., and Ando, Y. (2016) Novel antibody for the treatment of transthyretin amyloidosis. *J. Biol. Chem.* **291,** 25096–25105 CrossRef Medline
33. Hazenberg, B. P., Limburg, P. C., Bijzet, J., and van Rijswijk, M. H. (1999) A quantitative method for detecting deposits of amyloid A protein in aspirated fat tissue of patients with arthritis. *Ann. Rheum. Dis.* **58,** 96–102 CrossRef Medline
34. Puchtler, H., Sweat, F., and Levine, M. (1962) On the binding of Congo red by amyloid. *J. Histochem. Cytochem.* **10,** 355–363 CrossRef